THE JOURNAL OF PHYSICAL CHEMISTRY C

Article

Cite This: J. Phys. Chem. C 2019, 123, 20325−20332

pubs.acs.org/JPCC

Capturing the Long-Lived Photogenerated Electrons in Au/TiO_2 upon UV or Visible Irradiation by Time-Resolved Infrared Spectroscopy

Published as part of The Journal of Physical Chemistry virtual special issue "Hai-Lung Dai Festschrift".

Xiaojuan Dai,[†] Zeqing Jiao,[†] Zehan Ma, Kunhui Liu, Chen Wang, and Hongmei Su*

College of Chemistry, Beijing Normal University, Beijing 100875, China

Supporting Information

ABSTRACT: Gold nanoparticle modifications for TiO_2 (Au/TiO_2) can extend the absorption wavelength from UV to visible (Vis) and enhance the photocatalytic performance, thus fueling increasing attention as an emerging photocatalysis strategy. To explore the plasmon-enhanced photocatalytic mechanism and directly unveil the intrinsic properties of Au/TiO_2, the decay kinetics of photoelectrons upon UV (355 nm) or Vis (532 nm) excitation are monitored by means of nanosecond time-resolved infrared spectroscopy, which is a unique tool offering observations without interference of the holes. Under UV irradiation, the longer lifetime of photoelectrons observed in Au/TiO_2 compared to that in bare TiO_2 provides unambiguous evidence for the enhanced charge separation by AuNPs. Under Vis irradiation, the long-lived (hundreds of microseconds) electrons produced by injection from AuNPs into TiO_2 upon plasmon excitation are here detected for the first time. Moreover, the effects of TiO_2 phase composition and the amount of AuNPs loading on the decay kinetics of long-lived photoelectrons are examined.

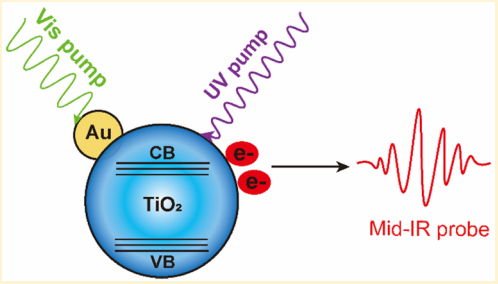

1. INTRODUCTION

Titanium dioxide (TiO_2) has been widely used and exhibits excellent photocatalytic performance in a wide range of fields, such as water splitting,[1] organic pollutant degradation, and selective organic synthesis.[2−6] Photocatalytic reaction takes place when TiO_2 is excited by energy larger than its band gap, resulting in the formation of electrons at the conduction band (CB) and holes at the valence band (VB).[7] However, there are two drawbacks greatly limiting its application in the field of photocatalysis. One is the rapid recombination rate of photoexcited charge carriers, which limits its activity.[8−10] The lifetime of the photogenerated electrons and holes is one important factor to determine the photocatalytic efficiency.[11] Another is the large band gap, ∼3.0 eV, which limits its absorption wavelength to shorter than 400 nm.[12−14] Considering that UV light accounts for only 3−5% of the overall energy of the sunlight reaching the earth's surface,[15] extension of its absorption wavelength range to the visible region to make full use of solar energy is an important issue. Up to now, many photocatalysis studies sought an effective way to eliminate the recombination of electrons and holes and a way to extend the wavelength range response.[8,16−19]

Numerous modifications have been performed to overcome the drawbacks of TiO_2, including doping with metallic or nonmetallic species,[20−23] coupling with a visible light sensitizer,[24−26] and fine-tuning the morphology.[27−32] Alternatively, loading noble metal, particularly gold nanoparticles (AuNPs) onto the surface of TiO_2, turns out to be one promising strategy. Modification of TiO_2 with AuNPs (Au/TiO_2) has been found to promote its photocatalytic activity upon UV excitation. The significant photocurrent and the suppressed photoluminescence (PL) emission suggested that the recombination of photogenerated electron−hole pairs can be inhibited by the accelerated transfer of photoexcited electrons from the CB of TiO_2 to AuNPs.[33−35] On the other hand, incorporation of AuNPs on the TiO_2 can extend the absorption wavelength of catalysts from UV to Vis because AuNPs exhibits a characteristic surface plasmon band in the visible-light region, owing to the collective excitation of electrons.[36] Upon Vis irradiation, the surface plasmon band of AuNPs is excited, and the generated excited electrons (hot electron) are injected into the empty CB of TiO_2.[14,37−39] Aside from being an effective approach to enhance photocatalytic activity, AuNPs are stable enough to resist corrosion under photocatalytic conditions and exhibit large optical absorption cross sections that can be manipulated throughout the solar spectrum.[38,40,41]

Mechanistically, what is the intrinsic reason that Au/TiO_2 can have such a better photocatalytic performance? Because the lifetime of electrons or holes determines whether they have more opportunities to react with the surface-adsorbed molecules, the recombination time of the photogenerated

Received: May 29, 2019
Revised: July 26, 2019
Published: July 27, 2019

DOI: 10.1021/acs.jpcc.9b05096
J. Phys. Chem. C 2019, 123, 20325−20332

electrons and holes can directly influence the photocatalytic activity. Thus, kinetics studies on the photogenerated charge carriers in Au/TiO_2 are essential for understanding the photocatalytic performance. However, it was difficult to identify the contribution of different carriers (electrons or holes) in the time-resolved UV−Vis spectra.[42] However, the photoelectron absorption in the mid-IR region has no interference of the holes. Therefore, time-resolved mid-IR absorption spectroscopy is potentially a powerful tool to accurately trace the kinetics of the photogenerated electrons.[43−45] UV excitation of bare TiO_2 resulted in a wide IR absorption spectrum from 3000 to 1000 cm^{-1}, which can be assigned to the optical transitions of electrons in the CB and/or from shallow midgap states.[46−49] The photoelectron IR absorption spectrum exhibits a fast decay in 1 μs followed by a slow decay lasting hundreds of microseconds. The fast decay is attributed to the recombination of electrons with free holes, while the slow decay is assigned to the recombination of electrons with trapped holes that are captured by surface hydroxyl groups.

Interestingly, the electron injection process from the AuNPs to the CB of the TiO_2 under Vis activation was investigated, which showed a high injection efficiency with a rate of dozens to hundreds of femtoseconds.[50−53] For the much slower recombination of active electrons and holes, however, the femtosecond time-resolved infrared (IR) probe transient spectroscopy study could only monitor the process lasting several nanoseconds.[51] The long-lived photogenerated electrons of Au/TiO_2 that drive photocatalytic reactions remain to be explored. Furthermore, it has been reported that the catalytic activity of Au/TiO_2 can be affected by the TiO_2 composition and the amount of AuNP loading;[54−56] whether these two factors will also influence the decay of photoelectrons has not been studied yet.

In this work, we perform nanosecond time-resolved IR spectroscopy measurements to investigate the decay kinetics of the photogenerated electrons in several Au/TiO_2 under respective UV (355 nm) or Vis (532 nm) laser irradiation. Our studies are focused on long-lived electrons in the microsecond time scale and the influence of different TiO_2 compositions and AuNP loadings. Under UV activation conditions, we find that the recombination rate of active electrons and holes is decelerated in Au/TiO_2 compared with that in bare TiO_2, which provides direct evidence for the enhanced charge separation by AuNPs. Under Vis activation conditions, we detect for the first time a slow decay of hundreds of microseconds for the photoelectrons in Au/TiO_2, demonstrating that the injected photoelectrons from AuNP plasmon excitation last long enough for photocatalytic reaction. It is further observed that the phase composition of TiO_2 and the amount of AuNP loading can affect the lifetime of photoelectrons under UV irradiation, while under Vis irradiation the injected electrons are not so sensitive to the composition of TiO_2. These results provide key kinetics data that directly reflect the intrinsic properties of Au/TiO_2 and are of great significance for understanding the photocatalysis mechanisms of Au/TiO_2.

2. MATERIALS AND METHODS

2.1. Materials. TiO_2 (P25, 80% anatase and 20% rutile) was purchased from Acros. Au/TiO_2 species, including AuNPs 1% on anatase/rutile mixed titania (1 wt % Au @ A/R TiO_2), AuNPs 1% on modified anatase titania (1 wt % Au @ mA TiO_2), gold 1% on titanium dioxide AUROlite (P25) (1 wt % Au @ P25),[57] AuNPs 10% on anatase/rutile mixed Titania (10 wt % Au @ A/R TiO_2), were all purchased from Strem corporation. Methylene blue (MB) was purchased from Alfa Aesar and used as received.

2.2. Steady-State Spectrum Measurement. Ultraviolet−visible (UV−Vis) transmittance and reflectance spectra were recorded using a UV−Vis spectrophotometer (UV-2600) equipped with an external diffuse reflectance accessory (DRA-2500), and the absorbance (A) was calculated using the formula $A = 1 - T - R$, where T is the total transmittance and R is the total reflectance.

2.3. Photocatalytic Activity Evaluation. Photocatalytic activities of TiO_2 (P25) and all the Au/TiO_2 under UV and Vis irradiation were evaluated by measuring the absorbance changes of the MB aqueous solution after 355 and 532 nm laser excitation. A certain amount of photocatalyst powder (2 mg) was added to 3 mL of a 1.6×10^{-5} mol/L MB aqueous solution in a 1 cm cuvette. The suspension solution was irradiated using a 355 and 532 nm laser with a light intensity of 10 mJ for a predetermined time. During the whole degradation process, the suspension was magnetically stirred to increase the contact between the catalyst and the solution. After the irradiation, the suspension was immediately centrifuged at 6000 rpm/min for 20 min to remove solids. Eventually, the residual concentration of MB in the supernatant was analyzed by using a UV−Vis spectrophotometer (U-3900, Hitachi, Japan) at the characteristic wavelength (λ_{MB} = 665 nm). To evaluate the photocatalytic activity, the degradation efficiency was obtained using eq 1

$$([MB]_0 - [MB])/[MB] = (A_0 - A)/A \quad (1)$$

where $[MB]_0$ and $[MB]$ are the concentrations of MB solution before and after UV irradiation. A_0 and A are the maximum absorbances of the MB solution at 665 nm before and after UV irradiation, respectively. All catalytic reactions were performed under air conditions.

2.4. Time-Resolved Fourier Transform IR (TR-FTIR) Experiment. Nanosecond time-resolved infrared absorption spectra were measured using a Bruker Vertex 80 V step scan FTIR spectrometer with an MCT detector, combined with a Nd:YAG laser (Spectra−Physics). There are two outputs from the detector: output DC, corresponding to the value of the static interferogram, and output AC, corresponding to the time-resolved change of the interferogram. An external fast ADC digitizer (Spectrum Instrumentation GmbH) was used to obtain a nanosecond time-resolved digital signal. The differential absorbance spectra were calculated based on the equation

$$\Delta A = A_{AC+DC} - A_{DC} = -\log_{10}(1 + \Delta I_{AC}/I_{DC})$$

where I_{DC} and ΔI_{AC} are the single-beam intensity spectra corresponding to static (DC) and dynamic (AC) channels. ΔI_{AC} was calibrated before being used in the equation because different gain was applied to the AC channel. The third and second harmonics of the Nd:YAG laser (355 and 532 nm) operating at a 10 Hz repetition rate were used in the experiments. The laser excitation beam was directed through an iris aperture (3 mm in diameter) and then overlapped with the infrared beam in the sample cell within the sample compartment of the FTIR spectrometer. The laser beam energy after the aperture was 1.5 mJ per pulse. Each catalyst

DOI: 10.1021/acs.jpcc.9b05096
J. Phys. Chem. C 2019, 123, 20325−20332

was fixed on a CaF_2 plate at 2−3 mg cm^{-2} and then placed in the compartment of the spectrometer. All TR-FTIR spectra were collected with a spectral resolution of 32 cm^{-1} under air conditions because the spectra and kinetics show little change in nitrogen, dry air, and the normal air.

3. RESULTS AND DISCUSSION

P25 and Au/TiO_2, including 1 wt % Au @ mA TiO_2, 1 wt % Au @ A/R TiO_2, 10 wt % Au @ A/R TiO_2, and 1 wt % Au @ P25, are chosen to study the kinetics of photoelectrons and explore the effect of AuNP loading and TiO_2 phase composition. As shown in the steady-state UV−Vis absorption spectra in Figure 1, bare TiO_2 (P25) mainly absorbs ultraviolet

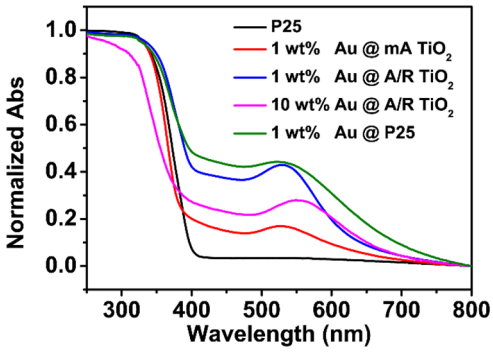

Figure 1. UV−Vis absorbance spectra of TiO_2 (P25) and Au/TiO_2 including 1 wt % Au @ mA TiO_2, 10 wt % Au @ A/R TiO_2, 1 wt % Au @ A/R TiO_2, and 1 wt % Au @ P25.

light less than 400 nm, while all Au/TiO_2 samples have absorption bands extended to the visible light range with maxima of around 550 nm, which is attributed to the plasmon resonance absorption of gold.[36] Therefore, we choose 355 and 532 nm lasers to excite Au/TiO_2 and study the catalytic performance and dynamics of photoelectrons under UV and Vis light irradiation, respectively.

3.1. Photocatalytic Activity Evaluated by Photodegrading Methylene Blue Aqueous Solution. To evaluate catalyst performance of P25 and Au/TiO_2, the photodegradation of the MB aqueous solution upon UV and Vis illumination was studied. Figure 2 shows the degradation efficiency of MB obtained with photocatalysts of P25 and several Au/TiO_2's upon 355 and 532 nm excitation by monitoring the absorption peak of MB at 665 nm in the steady-state UV−Vis spectra (Figure S1). Without catalyst, when the MB aqueous solution was exposed to a 355 or 532 nm laser, the decrease of the MB concentration was negligible, indicating that there is no background photoreaction of MB. In the presence of catalyst (P25 and Au/TiO_2), the degradation of MB becomes remarkable, which is obviously caused by the photocatalysis reaction. As shown in Figure 2a, the degradation efficiency of MB increases obviously in the presence of each catalyst in the order of 10 wt % Au @ A/R TiO_2 > 1 wt % Au @ P25 > 1 wt % Au @ A/R TiO_2 > P25 > 1 wt % Au @ mA TiO_2.

To compare with each other, the catalytic performance of 1 wt % Au @ P25 is better than that of bare P25, indicating that the loading of AuNPs indeed can enhance the photocatalytic ability of TiO_2, as reported before.[58] Additionally, both 1 wt % Au @ P25 and 1 wt % Au @ A/R TiO_2 can degrade more MB than 1 wt % Au @ mA TiO_2. This is consistent with the

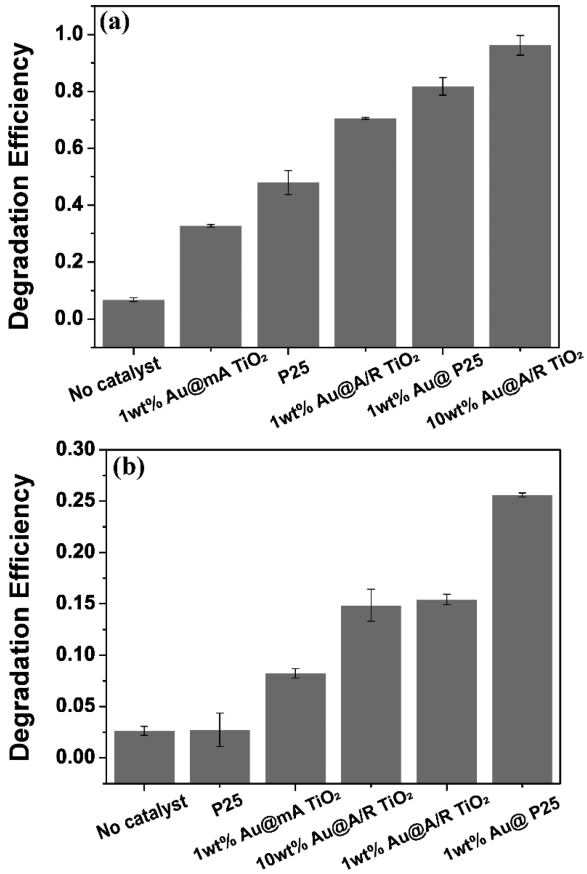

Figure 2. Degradation efficiency of a MB aqueous solution with P25 and Au/TiO_2 photocatalysts for a predetermined time: (a) after 355 nm laser irradiation and (b) after 532 nm laser irradiation.

previous reports for pure TiO_2,[54,59,60] indicating that the anatase/rutile mixed phase TiO_2, such as P25, has better photocatalytic activity than TiO_2 with a sole anatase or rutile phase. Moreover, the photocatalytic activity of 10 wt % Au @ A/R TiO_2 is better than that of 1 wt % Au @ A/R TiO_2, which may be attributed to the loading of a larger amount of AuNPs.

As shown in Figure 2b, there is approximately no degradation when MB is exposed alone to the 532 nm laser or in the presence of P25, which is reasonable because both MB itself and P25 have negligible absorption at 532 nm. For Au/TiO_2, thanks to the plasmon resonance absorption of gold, they all have a strong absorption at 532 nm; thus, they can be excited, and then the generated excited electrons (hot electron) transfer to TiO_2,[50] causing degradation of MB. Under Vis irradiation, AuNPs loaded on a mixture of anatase/rutile TiO_2 particles also have better MB degradation efficiencies, comparing the results of 1 wt % Au @ P25 and 1 wt % Au @ A/R TiO_2 with that of 1 wt % Au @ mA TiO_2.

3.2. Decay Kinetics of the Photoelectrons in Au/TiO_2 under UV and Vis Irradiation. After addressing the distinct photocatalysis performance of Au/TiO_2, we performed TR-FTIR measurements to monitor the photoelectron dynamics of these catalysts. Figure 3 shows the transient IR absorption spectra of P25 obtained after the nanosecond 355 nm laser irradiation. Immediately after UV excitation of bare TiO_2 (P25), a broad structureless absorption with monotonically increased intensity from 2500 to 1000 cm^{-1} is observed, which is the typical mid-IR absorption feature due to the optical transitions of electrons in the CB and/or from shallow midgap

DOI: 10.1021/acs.jpcc.9b05096
J. Phys. Chem. C 2019, 123, 20325−20332

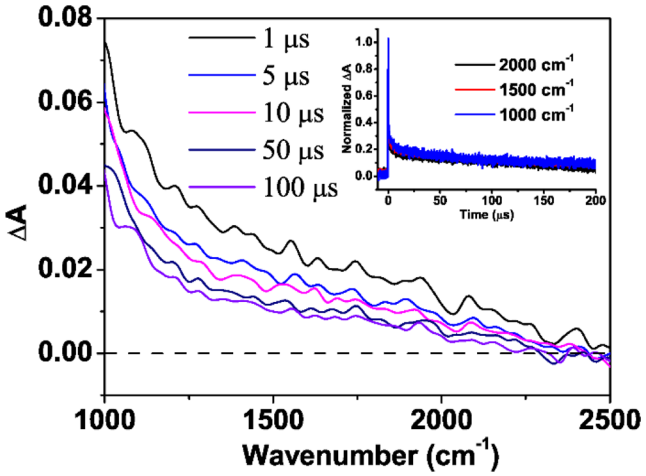

Figure 3. Time-resolved IR absorption spectra of P25 recorded at typical delay times after 355 nm laser pulse irradiation. The inset shows the normalized decay curves at 1000, 1500, and 2000 cm^{-1}.

states.[47] The inset of Figure 3 shows the decay curves at three selected wavenumbers of 1000, 1500, and 2000 cm^{-1}, which are identical indeed after normalization. Under the same condition, all of the Au/TiO_2 catalysts show similar transient IR absorption spectra (Figure S2), which are attributed to the photoelectrons of TiO_2 produced by exciting TiO_2 directly at 355 nm.

The decay curves of the photogenerated electrons in each Au/TiO_2 were traced at 2000 cm^{-1}. As shown in Figure 4, the

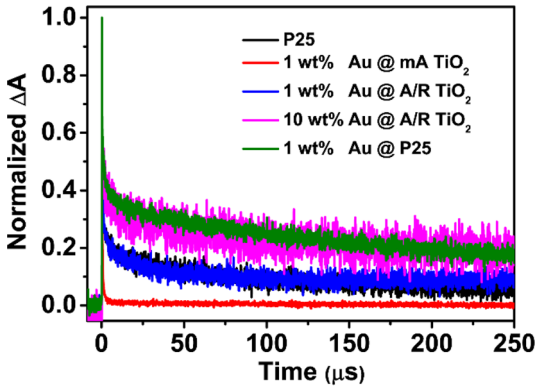

Figure 4. Normalized decay curves of transient IR absorption at 2000 cm^{-1} for the photoelectrons in P25 and different Au/TiO_2 catalysts upon excitation by the 355 nm laser.

transient IR absorption of P25 and all of the Au/TiO_2 except 1 wt % Au @ mA TiO_2 exhibits a fast decay in 1 μs initially and then a slow decay in hundreds of microseconds. According to the previous reports for the bare TiO_2 or platinized TiO_2,[44−48] the fast decay is mainly due to recombination of the electrons with the free holes, and the slow decay is ascribed to recombination of electrons with the trapped holes captured by surface hydroxyl groups. The slow decay component corresponds to the long-lived photoelectrons, which have increased lifetimes in the order of 1 wt % Au @ mA TiO_2 < P25 = 1 wt % Au @ A/R TiO_2 < 1 wt % Au @ P25 = 10 wt % Au @ A/R TiO_2, which is in general agreement with the catalyst's ability to degrade MB. Thus, the slowly recombined photoelectrons and holes are indeed correlated with the catalytic activity.

The decay of photoelectrons in 1 wt % Au @ P25 is slower than that in P25, which proves clearly that the photoelectrons produced by exciting P25 can be trapped by AuNPs and thus its recombination with a hole is suppressed. Additionally, the photoelectrons in 1 wt % Au @ mA TiO_2 decay to the baseline within 10 μs, which is much faster than the photoelectrons in 1 wt % Au @ A/R TiO_2 and 1 wt % Au @ P25 (hundreds of microseconds). The different phase composition of TiO_2 may be responsible for the much different photoelectron lifetime. In fact, it has been reported that P25 and other anatase/rutile mixed phase TiO_2 are more active than the TiO_2 sole phase in photocatalytic reactions, which is ascribed to the improved charge separation by electron transfer between the anatase and rutile phases in the mixed phase TiO_2, and the electron transfer percentage highly depends on the phase composition and anatase−rutile interface in mixed phase TiO_2.[34] Therefore, we're more inclined to think that the longer lifetimes of photoelectrons in 1 wt % Au @ A/R TiO_2 and 1 wt % Au @ P25 are mainly attributed to the improved charge separation of photogenerated carriers by charge transfer between anatase and rutile phase TiO_2. The different performance between 1 wt % Au @ A/R TiO_2 and 1 wt % Au @ P25 may be caused by the different composition ratio of anatase and rutile phases. Finally, the photoelectrons in 10 wt % Au @ A/R TiO_2 show a longer lifetime than those in 1 wt % Au @ A/R TiO_2, which provides a clear explanation for the better photocatalytic reactions of 10 wt % Au @ A/R TiO_2 compared to those of 1 wt % Au @ A/R TiO_2. It indicates that 10% AuNP loading can trap more electrons from TiO_2 than 1% AuNP loading. In short, the transient IR spectra reveal clearly the microsecond scale decay dynamics of photogenerated electrons in Au/TiO_2 under UV irradiation conditions. This gives direct evidence to demonstrate that AuNPs can prevent the recombination of active electrons and holes of TiO_2 and thus lead to long-lived electrons. In addition, the results suggest that the degree of separation of photogenerated carriers is affected by the TiO_2 composition and AuNP loading amount.

Upon illumination with a 532 nm laser, the bare TiO_2 (P25) cannot be excited; thus, it does not have any transient IR absorption signal (not shown). However, all of the Au/TiO_2 catalysts upon 532 nm excitation display a structureless and broad IR absorption spectrum with monotonically increased intensity from 2500 to 1000 cm^{-1} (Figure 5). This spectral feature resembles that of TiO_2 and Au/TiO_2 under 355 nm irradiation in general, although the overall signal is weaker. Moreover, it is known that photoexcitation of AuNPs cannot produce any infrared signal.[61] Thus, these broad IR absorptions are ascribed to the photoelectrons of TiO_2, which should be injected from the excited AuNPs upon 532 nm excitation (Scheme 1). The electron injection process from the AuNPs to the CB of the TiO_2 under Vis activation has been shown to be highly efficient with a rate of dozens to hundreds of femtoseconds.[50−53] The injected electrons then undergo recombination with the holes in AuNPs (Scheme 1). There is a fast decay within the nanosecond time scale,[51,62] which is attributed to the injected electrons' transfer back to AuNPs. The decay is strongly dependent on the position where the electron reached the TiO_2 surface. In addition, it was also discussed that in the femtosecond laser-pumped conditions a large number of injected electrons were produced, causing a trap filling effect, and charge recombination should be limited by electron diffusion in the CB of TiO_2 but not in the trapping states.[51] However, under weak light irradiation, no

DOI: 10.1021/acs.jpcc.9b05096
J. Phys. Chem. C 2019, 123, 20325−20332

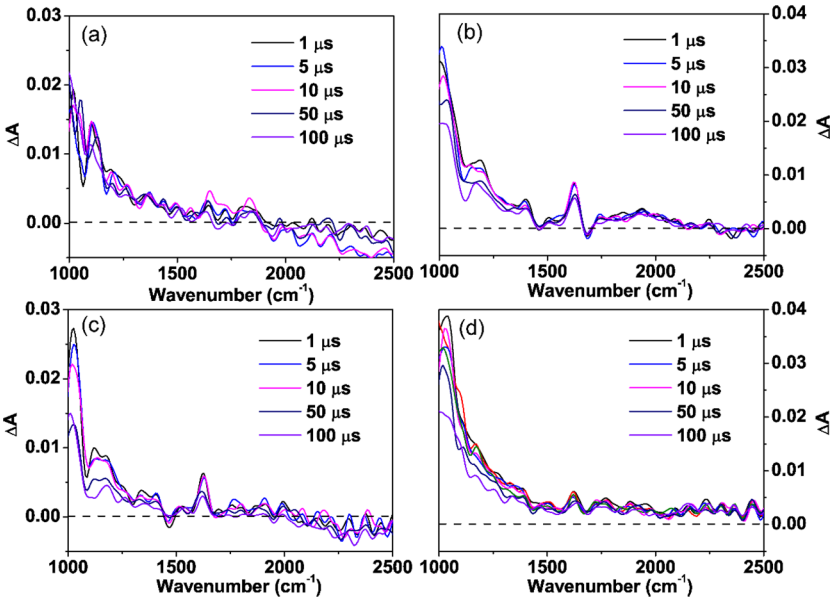

Figure 5. Time-resolved IR absorption spectra of Au/TiO_2 recorded at typical delay times after 532 nm laser pulse irradiation: (a) 1 wt % Au @ A/R TiO_2; (b) 1 wt % Au @ mA TiO_2; (c) 10 wt % Au @ A/R TiO_2; (d) 1 wt % Au @ P25.

Scheme 1. Energy Level Diagram Illustrating Electron Transfer and the Recombination Process under UV (a) and Vis (b) Irradiation[a]

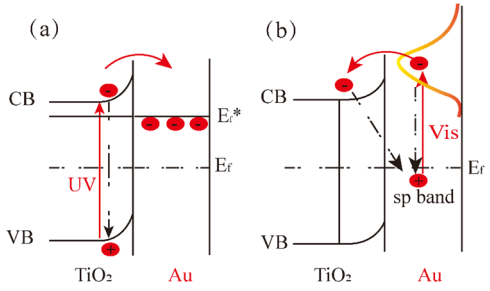

[a] E_f is the Fermi energy of AuNPs. E_f* represents the equilibrium Fermi level after negative shifting due to the accumulation of electrons. It's reported that this negative shift in E_f leads to better charge separation.[69].

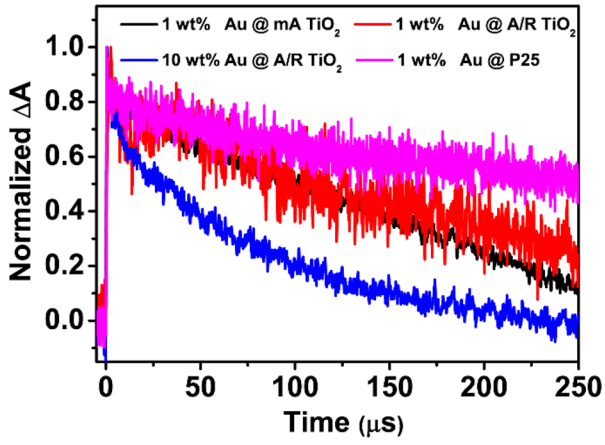

Figure 6. Normalized decay curves of transient IR absorption at 1200 cm^{-1} for the photoelectrons in P25 and different Au/TiO_2 catalysts upon excitation by a 532 nm laser.

trap filling effect is expected, and it will make the system have a longer lifetime, as in the case of dye-sensitized TiO_2, in which the electron lifetime is more than nanoseconds or even microseconds.[51] Because the longest time scale for the femtosecond laser-based IR detection can reach only nanoseconds, whether there exist long-lived hot electrons remains to be explored. The time window of our nanosecond time-resolved FTIR measurements is nanoseconds to milliseconds, which allows detection of longer-lived electrons.

Here, a slow decay process of the injected photoelectrons of Au/TiO_2 is observed in the nanosecond time-resolved FTIR spectra, as evidenced by the kinetics curves of the transient IR absorptions at 1200 cm^{-1} (Figure 6). The decay of these long-lived photoelectrons lasts until 250 μs. The nonexponential kinetics may be due to diffusion of many electrons within the TiO_2 particles[50] or a wide distribution of trap sites.[63] Apart from being accumulated in the CB, the injected hot electrons also have the opportunity to diffuse and become trapped at various electronic states within the TiO_2, whose energy levels are lower than those of the CB.[15] Most likely, the hundreds of microseconds slow decay observed here can be attributed to the electrons trapped farther away from AuNPs at some shallow midgap states of TiO_2. Those electrons in shallow traps exhibit lifetimes of hundreds of microseconds, which is similar to the case of dye-sensitized TiO_2.[25] In addition to back electron transfer, the shallow trap electrons can also decay to other deep trap sites of TiO_2. The electrons in deep trap sites of TiO_2 may have absorption in the near-IR region at around 7500 cm^{-1}, as in the case of dye-sensitized TiO_2,[25] but it is out of the spectral window of the current mid-IR detection. The deep trap electrons such as at oxygen vacancies for Au/TiO_2 may have much longer lifetimes of minutes, as reported by an electron paramagnetic resonance (EPR) measurement.[64]

For the catalysts of 1 wt % Au @ P25, 1 wt % Au @ A/R TiO_2, and 1 wt % Au @ mA TiO_2, the decay rates of the long-lived photoelectrons are similar. This indicates that under Vis irradiation the recombination of photoelectrons with the holes in the AuNPs is not so sensitive to the TiO_2 phase structure. This is probably because the electrons are injected from

DOI: 10.1021/acs.jpcc.9b05096
J. Phys. Chem. C 2019, 123, 20325−20332

excited AuNPs but not directly produced by excitation of TiO_2 as under UV light. To inspect closely, the lifetime of photoelectrons in 1 wt % Au @ P25 appears to be the longest. Meanwhile, the strongest photoelectron signals are seen for 1 wt % Au @ P25 (Figure 5d), which indicates formation of a larger number of photoelectrons. The longest lifetime and the strongest photoelectron signal are both consistent with the better ability to degrade MB for this catalyst (Figure 2b). The photoelectrons in 10 wt % Au @ A/R TiO_2 decay obviously faster than that in 1 wt % Au @ A/R TiO_2, which may be associated with the increasing density of states caused by the larger amount of AuNPs or the presence of Au aggregates, as indicated by the red shift of the plasmonic band in the UV−Vis spectra (Figure 1). However, there is stronger photoelectron signal observed for 10 wt % Au @ A/R TiO_2 compared to that of 1 wt % Au @ A/R TiO_2 (see Figure 5a,c), which can compensate the shorter photoelectron lifetime. Therefore, the net photocatalysis result to degrade MB turns out to be similar for the two catalysts of 10 wt % Au @ A/R TiO_2 and 1 wt % Au @ A/R TiO_2.

Overall, for Au/TiO_2 under Vis excitation, the efficiency of the long-lived photoelectrons produced by injection is not as high as that for direct UV excitation; therefore, the photoelectron signal intensity and the photocatalysis ability under 532 nm irradiation are weaker than those in the case of direct irradiation by a 355 nm laser. This may also be the reason why the consistency between the lifetime of photoelectrons and the ability to degrade MB is not as good as the situation under UV irradiation. However, considering the long lifetime of photoelectrons observed here and the ultrafast injection rate reported before, these two factors still guarantee the promising photocatalytic ability of Au/TiO_2 under visible light irradiation. According to previous research, the reaction sites for plasmonic holes are mainly distributed on the AuNPs and the interface, while the reaction sites for electrons are distributed on the TiO_2 surface.[65] The photocatalytic degradation of MB here involves the participation of both electrons and holes.[66]

The schematic electron transfer and recombination processes are depicted in Scheme 1. Upon 355 nm laser irradiation, the electrons at the VB of TiO_2 are elevated to the CB band and then transferred to AuNPs because the Fermi level of the AuNPs is lower than the CB level.[35] Therefore, AuNPs facilitate the separation of electrons and holes and decrease their recombination rate. The long-lived electrons have more opportunities to react with the surface-adsorbed molecules to enhance the photocatalytic performance. Upon 532 nm laser irradiation, AuNPs are photoexcited through the SPR absorption, and then, the plasmon-excited hot electrons with sufficient energy can be injected efficiently into the CB of TiO_2 after overcoming the Schottky barrier (~1.0 eV), which is a natural result caused by the contact of noble metal NPs with the semiconductor photocatalyst.[67,68] The formation of a Schottky barrier can enhance the separation of electrons and holes, which in turn can reduce the recombination rate and increase the lifetime of charge carriers.

Our TR-FTIR experiments provide kinetics data for the slower decay of photoelectrons after modifying AuNPs on the TiO_2 under either UV or Vis irradiation. The existence of long-lived electrons of Au/TiO_2 under UV irradiation is proved directly. In addition, the slow decay kinetics of the injected photoelectrons in Au/TiO_2 under Vis irradiation is detected. Our experiments show that the long-lived electrons on the time scale of hundreds of microseconds in Au/TiO_2 can be produced under both UV and Vis irradiation. Therefore, the surface-modified TiO_2 with AuNPs can effectively overcome the limitations of TiO_2 itself, including slowing down the recombination of charge carriers and extending the photocatalytic capacity of TiO_2 to the visible region.

4. CONCLUSIONS

In this work, we used time-resolved FTIR spectroscopy to investigate the decay kinetics of the photogenerated electrons of several typical Au/TiO_2 under either UV (355 nm) or Vis (532 nm) irradiation. For the case of 355 nm laser irradiation, it is clearly shown that the recombination of photoelectrons with holes of TiO_2 is suppressed by AuNPs. For the case of 532 nm laser irradiation, we find that the electrons injected into TiO_2 after excitation of AuNPs survive a long time, and the long-lived (hundreds of microseconds) photoelectrons are observed and characterized in the transient IR spectra for the first time. Moreover, the TR-FTIR results reveal that these long-lived photogenerated electrons can be affected by the amount of AuNP loading under both UV and Vis conditions. In terms of the phase composition of TiO_2, it affects the photogenerated electrons under UV conditions, while under Vis conditions the injected photoelectrons are not so sensitive to the phase composition, depending on whether TiO_2 is directly excited or not. These findings provide essential kinetics information for better understanding of the photocatalytic performance and plasmon-enhanced photocatalytic mechanisms of Au/TiO_2 under either UV or Vis irradiation, which is of critical importance for rational design of Au/TiO_2 photocatalysts with high performance and utilization of visible light in solar energy.

■ ASSOCIATED CONTENT

Supporting Information

The Supporting Information is available free of charge on the ACS Publications website at DOI: 10.1021/acs.jpcc.9b05096.

UV−Vis absorption spectra of a methylene blue aqueous solution with P25 and Au/TiO_2 photocatalysts upon 355 and 532 nm excitation and TR-FTIR spectra of Au/TiO_2 under 355 nm laser irradiation (PDF)

■ AUTHOR INFORMATION

Corresponding Author

*E-mail: hongmei@bnu.edu.cn or hongmei@iccas.ac.cn.

ORCID

Hongmei Su: 0000-0001-7384-6523

Author Contributions

†X.D. and Z.J. contributed equally.

Notes

The authors declare no competing financial interest.

■ ACKNOWLEDGMENTS

This work is financially supported by the National Natural Science Foundation of China (Grant No. 21425313, 21727803, and 21803008)

■ REFERENCES

(1) Fujishima, A.; Honda, K. Electrochemical Photolysis of Water at a Semiconductor Electrode. *Nature* **1972**, *238*, 37−38.

DOI: 10.1021/acs.jpcc.9b05096
J. Phys. Chem. C 2019, 123, 20325−20332

(2) Linsebigler, A. L.; Lu, G.; Yates, J. T. Photocatalysis on TiO_2 Surfaces: Principles, Mechanisms, and Selected Results. *Chem. Rev.* **1995**, *95*, 735−758.
(3) Hoffmann, M. R.; Martin, S. T.; Choi, W.; Bahnemann, D. W. Environmental Applications of Semiconductor Photocatalysis. *Chem. Rev.* **1995**, *95*, 69−96.
(4) Chen, X.; Mao, S. S. Titanium Dioxide Nanomaterials: Synthesis, Properties, Modifications, and Applications. *Chem. Rev.* **2007**, *107*, 2891−2959.
(5) Liu, L.; Chen, X. Titanium Dioxide Nanomaterials: Self-Structural Modifications. *Chem. Rev.* **2014**, *114*, 9890−9918.
(6) Dahl, M.; Liu, Y.; Yin, Y. Composite Titanium Dioxide Nanomaterials. *Chem. Rev.* **2014**, *114*, 9853−9889.
(7) Bai, S.; Jiang, J.; Zhang, Q.; Xiong, Y. Steering Charge Kinetics in Photocatalysis: Intersection of Materials Syntheses, Characterization Techniques and Theoretical Simulations. *Chem. Soc. Rev.* **2015**, *44*, 2893−2939.
(8) Asahi, R.; Morikawa, T.; Ohwaki, T.; Aoki, K.; Taga, Y. Visible-Light Photocatalysis in Nitrogen-Doped Titanium Oxides. *Science* **2001**, *293*, 269−271.
(9) Yu, J. C.; Yu; Ho; Jiang; Zhang. Effects of F^- Doping on the Photocatalytic Activity and Microstructures of Nanocrystalline TiO_2 Powders. *Chem. Mater.* **2002**, *14*, 3808−3816.
(10) Shimizu, K.-i.; Itoh, S.; Hatamachi, T.; Kodama, T.; Sato, M.; Toda, K. Photocatalytic Water Splitting on Ni-Intercalated Ruddlesden−Popper Tantalate $H_2La_{2/3}Ta_2O_7$. *Chem. Mater.* **2005**, *17*, 5161−5166.
(11) Amano, F.; Yamakata, A.; Nogami, K.; Osawa, M.; Ohtani, B. Visible Light Responsive Pristine Metal Oxide Photocatalyst: Enhancement of Activity by Crystallization under Hydrothermal Treatment. *J. Am. Chem. Soc.* **2008**, *130*, 17650−17651.
(12) Ohno, T.; Sarukawa, K.; Tokieda, K.; Matsumura, M. Morphology of a TiO_2 Photocatalyst (Degussa, P-25) Consisting of Anatase and Rutile Crystalline Phases. *J. Catal.* **2001**, *203*, 82−86.
(13) Schneider, J.; Matsuoka, M.; Takeuchi, M.; Zhang, J.; Horiuchi, Y.; Anpo, M.; Bahnemann, D. W. Understanding TiO_2 Photocatalysis: Mechanisms and Materials. *Chem. Rev.* **2014**, *114*, 9919−9986.
(14) Wang, Z.; Liu, Y.; Huang, B.; Dai, Y.; Lou, Z.; Wang, G.; Zhang, X.; Qin, X. Progress on Extending The Light Absorption Spectra of Photocatalysts. *Phys. Chem. Chem. Phys.* **2014**, *16*, 2758−2774.
(15) Zhang, Y.; He, S.; Guo, W.; Hu, Y.; Huang, J.; Mulcahy, J. R.; Wei, W. D. Surface-Plasmon-Driven Hot Electron Photochemistry. *Chem. Rev.* **2018**, *118*, 2927−2954.
(16) Cho, Y.; Choi, W. Visible Light-Induced Reactions of Humic Acids on TiO_2. *J. Photochem. Photobiol., A* **2002**, *148*, 129−135.
(17) Kosowska, B.; Mozia, S.; Morawski, A. W.; Grzmil, B.; Janus, M.; Kałucki, K. The Preparation of TiO_2−Nitrogen Doped by Calcination of $TiO_2 \cdot xH_2O$ under Ammonia Atmosphere for Visible Light Photocatalysis. *Sol. Energy Mater. Sol. Cells* **2005**, *88*, 269−280.
(18) Zaleska, A.; Górska, P.; Sobczak, J. W.; Hupka, J. Thioacetamide and Thiourea Impact on Visible Light Activity of TiO_2. *Appl. Catal., B* **2007**, *76*, 1−8.
(19) Wang, J.; Tafen, D. N.; Lewis, J. P.; Hong, Z.; Manivannan, A.; Zhi, M.; Li, M.; Wu, N. Origin of Photocatalytic Activity of Nitrogen-Doped TiO_2 Nanobelts. *J. Am. Chem. Soc.* **2009**, *131*, 12290−12297.
(20) Christopher, P.; Ingram, D. B.; Linic, S. Enhancing Photochemical Activity of Semiconductor Nanoparticles with Optically Active Ag Nanostructures: Photochemistry Mediated by Ag Surface Plasmons. *J. Phys. Chem. C* **2010**, *114*, 9173−9177.
(21) Salehifar, N.; Nikfarjam, A. Improvement the Visible Light Photocatalytic Activity of Gold Nanoparticle, Co_2O_3 and Nitrogen Doped TiO_2 Nanofibers. *Mater. Lett.* **2017**, *188*, 59−62.
(22) Yang, K.-S.; Lu, Y.-R.; Hsu, Y.-Y.; Lin, C.-J.; Tseng, C.-M.; Liou, S. Y. H.; Kumar, K.; Wei, D.-H.; Dong, C.-L.; Chen, C.-L. Plasmon-Induced Visible-Light Photocatalytic Activity of Au Nanoparticle-Decorated Hollow Mesoporous TiO_2: A View by X-ray Spectroscopy. *J. Phys. Chem. C* **2018**, *122*, 6955−6962.
(23) Seh, Z. W.; Liu, S.; Low, M.; Zhang, S.-Y.; Liu, Z.; Mlayah, A.; Han, M.-Y. Janus Au-TiO_2 Photocatalysts with Strong Localization of Plasmonic Near-Fields for Efficient Visible-Light Hydrogen Generation. *Adv. Mater.* **2012**, *24*, 2310−2314.
(24) Katoh, R.; Furube, A.; Yoshihara, T.; Hara, K.; Fujihashi, G.; Takano, S.; Murata, S.; Arakawa, H.; Tachiya, M. Efficiencies of Electron Injection from Excited N_3 Dye into Nanocrystalline Semiconductor (ZrO_2, TiO_2, ZnO, Nb_2O_5, SnO_2, In_2O_3) Films. *J. Phys. Chem. B* **2004**, *108*, 4818−4822.
(25) Takeshita, K.; Sasaki, Y.; Kobashi, M.; Tanaka, Y.; Maeda, S.; Yamakata, A.; Ishibashi, T.-a.; Onishi, H. Effect of Annealing Temperature on Back Electron Transfer and Distribution of Deep Trap Sites in Dye-Sensitized TiO_2, Studied by Time-Resolved Infrared Spectroscopy. *J. Phys. Chem. B* **2004**, *108*, 2963−2969.
(26) Martini, I.; Hodak, J. H.; Hartland, G. V. Dynamics of Semiconductor-to-Dye Electron Transfer for Anthracene Dyes Bound to Different Sized TiO_2 Particles. *J. Phys. Chem. B* **1999**, *103*, 9104−9111.
(27) Chen, X.; Liu, L.; Huang, F. Black Titanium Dioxide (TiO_2) Nanomaterials. *Chem. Soc. Rev.* **2015**, *44*, 1861−1885.
(28) Rahman, Z. U.; Wei, N.; Feng, Y.; Zhang, X.; Wang, D. Synthesis of Hollow Mesoporous TiO_2 Microspheres with Single and Double Au Nanoparticle Layers for Enhanced Visible-Light Photocatalysis. *Chem. - Asian J.* **2018**, *13*, 432−439.
(29) Du, J.; Qi, J.; Wang, D.; Tang, Z. Facile Synthesis of Au@TiO_2 Core−Shell Hollow Spheres for Dye-Sensitized Solar Cells with Remarkably Improved Efficiency. *Energy Environ. Sci.* **2012**, *5*, 6914−6918.
(30) Li, J.; Zeng, H. C. Size Tuning, Functionalization, and Reactivation of Au in TiO_2 Nanoreactors. *Angew. Chem., Int. Ed.* **2005**, *44*, 4342−4345.
(31) Wu, X.-F.; Song, H.-Y.; Yoon, J.-M.; Yu, Y.-T.; Chen, Y.-F. Synthesis of Core−Shell Au@TiO_2 Nanoparticles with Truncated Wedge-Shaped Morphology and Their Photocatalytic Properties. *Langmuir* **2009**, *25*, 6438−6447.
(32) Wang, X. D.; Graugnard, E.; King, J. S.; Wang, Z. L.; Summers, C. J. Large-Scale Fabrication of Ordered Nanobowl Arrays. *Nano Lett.* **2004**, *4*, 2223−2226.
(33) Li, H.; Bian, Z.; Zhu, J.; Huo, Y.; Li, H.; Lu, Y. Mesoporous Au/TiO_2 Nanocomposites with Enhanced Photocatalytic Activity. *J. Am. Chem. Soc.* **2007**, *129*, 4538−4539.
(34) Stevanovic, A.; Ma, S.; Yates, J. T. Effect of Gold Nanoparticles on Photoexcited Charge Carriers in Powdered TiO_2−Long Range Quenching of Photoluminescence. *J. Phys. Chem. C* **2014**, *118*, 21275−21280.
(35) Subramanian, V.; Wolf, E. E.; Kamat, P. V. Catalysis with TiO_2/Gold Nanocomposites. Effect of Metal Particle Size on the Fermi Level Equilibration. *J. Am. Chem. Soc.* **2004**, *126*, 4943−4950.
(36) Primo, A.; Corma, A.; García, H. Titania Supported Gold Nanoparticles as Photocatalyst. *Phys. Chem. Chem. Phys.* **2011**, *13*, 886−910.
(37) Tian, Y.; Tatsuma, T. Mechanisms and Applications of Plasmon-Induced Charge Separation at TiO_2 Films Loaded with Gold Nanoparticles. *J. Am. Chem. Soc.* **2005**, *127*, 7632−7637.
(38) Linic, S.; Christopher, P.; Ingram, D. B. Plasmonic-metal Nanostructures for Efficient Conversion of Solar to Chemical Energy. *Nat. Mater.* **2011**, *10*, 911.
(39) Wu, K.; Chen, J.; McBride, J. R.; Lian, T. Efficient Hot-Electron Transfer by A Plasmon-Induced Interfacial Charge-Transfer Transition. *Science* **2015**, *349*, 632.
(40) Pelton, M.; Aizpurua, J.; Bryant, G. Metal-Nanoparticle Plasmonics. *Laser Photonics Rev.* **2008**, *2*, 136−159.
(41) Giannini, V.; Fernández-Domínguez, A. I.; Heck, S. C.; Maier, S. A. Plasmonic Nanoantennas: Fundamentals and Their Use in Controlling the Radiative Properties of Nanoemitters. *Chem. Rev.* **2011**, *111*, 3888−3912.
(42) Yoshihara, T.; Katoh, R.; Furube, A.; Tamaki, Y.; Murai, M.; Hara, K.; Murata, S.; Arakawa, H.; Tachiya, M. Identification of Reactive Species in Photoexcited Nanocrystalline TiO_2 Films by

DOI: 10.1021/acs.jpcc.9b05096
J. Phys. Chem. C 2019, 123, 20325−20332

Wide-Wavelength-Range (400−2500 nm) Transient Absorption Spectroscopy. *J. Phys. Chem. B* **2004**, *108*, 3817−3823.
(43) Yamakata, A.; Ishibashi, T.-a.; Onishi, H. Time-resolved Infrared Absorption Study of Nine TiO_2 Photocatalysts. *Chem. Phys.* **2007**, *339*, 133−137.
(44) Chen, T.; Feng, Z.; Wu, G.; Shi, J.; Ma, G.; Ying, P.; Li, C. Mechanistic Studies of Photocatalytic Reaction of Methanol for Hydrogen Production on Pt/TiO_2 by in situ Fourier Transform IR and Time-Resolved IR Spectroscopy. *J. Phys. Chem. C* **2007**, *111*, 8005−8014.
(45) Shen, S.; Wang, X.; Chen, T.; Feng, Z.; Li, C. Transfer of Photoinduced Electrons in Anatase−Rutile TiO_2 Determined by Time-Resolved Mid-Infrared Spectroscopy. *J. Phys. Chem. C* **2014**, *118*, 12661−12668.
(46) Yamakata, A.; Ishibashi, T.-a.; Onishi, H. Time-resolved Infrared Absorption Spectroscopy of Photogenerated Electrons in Platinized TiO_2 Particles. *Chem. Phys. Lett.* **2001**, *333*, 271−277.
(47) Yamakata, A.; Ishibashi, T.-a.; Onishi, H. Water- and Oxygen-Induced Decay Kinetics of Photogenerated Electrons in TiO_2 and Pt/TiO_2: A Time-Resolved Infrared Absorption Study. *J. Phys. Chem. B* **2001**, *105*, 7258−7262.
(48) Yamakata, A.; Ishibashi, T.-a.; Onishi, H. Electron- and Hole-Capture Reactions on Pt/TiO_2 Photocatalyst Exposed to Methanol Vapor Studied with Time-Resolved Infrared Absorption Spectroscopy. *J. Phys. Chem. B* **2002**, *106*, 9122−9125.
(49) Yamakata, A.; Ishibashi, T.-a.; Onishi, H. Kinetics of The Photocatalytic Water-Splitting Reaction on TiO_2 and Pt/TiO_2 Studied by Time-Resolved Infrared Absorption Spectroscopy. *J. Mol. Catal. A: Chem.* **2003**, *199*, 85−94.
(50) Furube, A.; Du, L.; Hara, K.; Katoh, R.; Tachiya, M. Ultrafast Plasmon-Induced Electron Transfer from Gold Nanodots into TiO_2 Nanoparticles. *J. Am. Chem. Soc.* **2007**, *129*, 14852−14853.
(51) Du, L.; Furube, A.; Yamamoto, K.; Hara, K.; Katoh, R.; Tachiya, M. Plasmon-Induced Charge Separation and Recombination Dynamics in Gold−TiO_2 Nanoparticle Systems: Dependence on TiO_2 Particle Size. *J. Phys. Chem. C* **2009**, *113*, 6454−6462.
(52) Du, L.; Furube, A.; Hara, K.; Katoh, R.; Tachiya, M. Ultrafast Plasmon Induced Electron Injection Mechanism in Gold−TiO_2 Nanoparticle System. *J. Photochem. Photobiol., C* **2013**, *15*, 21−30.
(53) Aiboushev, A.; Gostev, F.; Shelaev, I.; Kostrov, A.; Kanaev, A.; Museur, L.; Traore, M.; Sarkisov, O.; Nadtochenko, V. Spectral Properties of The Surface Plasmon Resonance and Electron Injection from Gold Nanoparticles to TiO_2 Mesoporous Film: Femtosecond Study. *Photochem. Photobiol. Sci.* **2013**, *12*, 631−637.
(54) Zhang, J.; Xu, Q.; Feng, Z.; Li, M.; Li, C. Importance of the Relationship between Surface Phases and Photocatalytic Activity of TiO_2. *Angew. Chem., Int. Ed.* **2008**, *47*, 1766−1769.
(55) Tsukamoto, D.; Shiraishi, Y.; Sugano, Y.; Ichikawa, S.; Tanaka, S.; Hirai, T. Gold Nanoparticles Located at the Interface of Anatase/Rutile TiO_2 Particles as Active Plasmonic Photocatalysts for Aerobic Oxidation. *J. Am. Chem. Soc.* **2012**, *134*, 6309−6315.
(56) Dong, W.; Reichenberger, S.; Chu, S.; Weide, P.; Ruland, H.; Barcikowski, S.; Wagener, P.; Muhler, M. The Effect of The Au Loading on The Liquid-Phase Aerobic Oxidation of Ethanol over Au/TiO_2 Catalysts Prepared by Pulsed Laser Ablation. *J. Catal.* **2015**, *330*, 497−506.
(57) Heeskens, D.; Aghaei, P.; Kaluza, S.; Strunk, J.; Muhler, M. Selective Oxidation of Ethanol in The Liquid Phase over Au/TiO_2. *Phys. Status Solidi B* **2013**, *250*, 1107−1118.
(58) Wada, N.; Yokomizo, Y.; Yogi, C.; Katayama, M.; Tanaka, A.; Kojima, K.; Inada, Y.; Ozutsumi, K. Effect of Adding Au Nanoparticles to TiO_2 Films on Crystallization, Phase Transformation, and Photocatalysis. *J. Mater. Res.* **2018**, *33*, 467−481.
(59) Ohno, T.; Tokieda, K.; Higashida, S.; Matsumura, M. Synergism between Rutile and Anatase TiO_2 Particles in Photocatalytic Oxidation of Naphthalene. *Appl. Catal., A* **2003**, *244*, 383−391.
(60) Li, G.; Ciston, S.; Saponjic, Z. V.; Chen, L.; Dimitrijevic, N. M.; Rajh, T.; Gray, K. A. Synthesizing Mixed-Phase TiO_2 Nanocomposites Using a Hydrothermal Method for Photo-Oxidation and Photoreduction Applications. *J. Catal.* **2008**, *253*, 105−110.
(61) Ratchford, D. C.; Dunkelberger, A. D.; Vurgaftman, I.; Owrutsky, J. C.; Pehrsson, P. E. Quantification of Efficient Plasmonic Hot-Electron Injection in Gold Nanoparticle−TiO_2 Films. *Nano Lett.* **2017**, *17*, 6047−6055.
(62) Bian, Z.; Tachikawa, T.; Zhang, P.; Fujitsuka, M.; Majima, T. Au/TiO_2 Superstructure-Based Plasmonic Photocatalysts Exhibiting Efficient Charge Separation and Unprecedented Activity. *J. Am. Chem. Soc.* **2014**, *136*, 458−465.
(63) Martini, I.; Hodak, J. H.; Hartland, G. V. Effect of Structure on Electron Transfer Reactions between Anthracene Dyes and TiO_2 Nanoparticles. *J. Phys. Chem. B* **1998**, *102*, 9508−9517.
(64) Priebe, J. B.; Karnahl, M.; Junge, H.; Beller, M.; Hollmann, D.; Brückner, A. Water Reduction with Visible Light: Synergy between Optical Transitions and Electron Transfer in Au-TiO_2 Catalysts Visualized by In situ EPR Spectroscopy. *Angew. Chem., Int. Ed.* **2013**, *52*, 11420−11424.
(65) Wang, S.; Gao, Y.; Miao, S.; Liu, T.; Mu, L.; Li, R.; Fan, F.; Li, C. Positioning the Water Oxidation Reaction Sites in Plasmonic Photocatalysts. *J. Am. Chem. Soc.* **2017**, *139*, 11771−11778.
(66) Wan, G.; Peng, X.; Zeng, M.; Yu, L.; Wang, K.; Li, X.; Wang, G. The Preparation of $Au@TiO_2$ Yolk−Shell Nanostructure and its Applications for Degradation and Detection of Methylene Blue. *Nanoscale Res. Lett.* **2017**, DOI: 10.1186/s11671-017-2313-4.
(67) Tang, J.; White, M.; Stucky, G. D.; McFarland, E. W. Electrochemical Fabrication of Large-Area Au/TiO_2 Junctions. *Electrochem. Commun.* **2003**, *5*, 497−501.
(68) McFarland, E. W.; Tang, J. A Photovoltaic Device Structure Based on Internal Electron Emission. *Nature* **2003**, *421*, 616−618.
(69) Jakob, M.; Levanon, H.; Kamat, P. V. Charge Distribution between UV-Irradiated TiO_2 and Gold Nanoparticles: Determination of Shift in the Fermi Level. *Nano Lett.* **2003**, *3*, 353−358.

DOI: 10.1021/acs.jpcc.9b05096
J. Phys. Chem. C 2019, 123, 20325−20332